

Enhancing BEMD decomposition using adaptive support size for CSRBF functions

Mohammed Arrazaki¹, Othman El Ouahabi², Mohamed Zohry¹, Adel Babbah³

¹Department of Mathematics, Faculty of Sciences, University AbdelMalek Essaadi, Tetouan, Morocco

²National School of Applied Sciences, University AbdelMalek Essaadi, Tangier, Morocco

³Department of Mathematics, Faculty of Polydisciplinary, University of AbdelMalek Essaadi, Larache, Morocco

Article Info

Article history:

Received Jul 27, 2024

Revised Oct 16, 2024

Accepted Oct 30, 2024

Keywords:

BEMD decomposition
 CSRBF functions
 Intrinsic mode functions
 Orthogonality index
 Synthetic texture image
 Time-frequency analysis
 Wendland functions

ABSTRACT

Despite their widespread development, the Fourier transform and wavelet transform are still unsuitable for analyzing non-stationary and non-linear signals. To address this limitation, bidimensional empirical mode decomposition (BEMD) has emerged as a promising technique. BEMD effectively extracts structures at various scales and frequencies but faces significant computational complexity, primarily during the extremum interpolation phase. To mitigate this, different interpolation functions were presented and suggested, with BEMD using compactly supported radial basis functions (BEMD-CSRBF) showing promising results in reducing computational cost while maintaining decomposition quality. However, the choice of support size for CSRBF functions significantly impacts the quality of BEMD. This article presents an enhancement to the BEMD-CSRBF algorithm by adjusting the CSRBF support size based on the extrema distribution of the image. Our method's results show a significant improvement in the BEMD-CSRBF algorithm's quality. Furthermore, when compared to the other two approaches to BEMD, it shows higher accuracy in terms of both intrinsic mode function (IMF) quality and computational efficiency.

This is an open access article under the [CC BY-SA](https://creativecommons.org/licenses/by-sa/4.0/) license.



Corresponding Author:

Mohammed Arrazaki

Department of Mathematics, Faculty of Sciences, University AbdelMalek Essaadi

BP. 2121 M'Hannech II, 93030 Tetouan, Morocco

Email: rezaki_mohamed@hotmail.com

1. INTRODUCTION

Huang *et al.* [1] introduced empirical mode decomposition (EMD) as an effective method for analyzing non-stationary and non-linear signals in one-dimensional (1D). It has been shown to be efficient for signal denoising [2]. The EMD approach has prompted researchers to develop the technique for bidimensional signals. The 2D extension of EMD was created by Nunes *et al.* [3], it is known as bidimensional empirical mode decomposition (BEMD), and it keeps the same concept as EMD via decomposition of an image to a set of intrinsic modal functions (IMFs) using an iterative process. This technique has made it possible to develop new methods in the analysis and processing of images that can be applied to any image, especially textured images, the results of which show better performance compared to existing decomposition techniques [3]. BEMD has been applied in different imaging areas such as texture analysis [4], [5], image indexing [6], image classification [7]–[10], image watermarking [11], [12], image segmentation [13], and fractal analysis [14]. The quality or performance of an IMF depends on the quality of preceding IMFs. The choice of the stopping criterion for the sifting process is therefore very important and is based on the following two conditions [3]:

- For each IMF, there are an equal number of zero crossings and extrema.
- Each IMF is symmetrical with respect to the local mean. In addition, the signal is assumed to have at least two extrema.

These conditions are by definition the properties of an IMF. The principle of the BEMD requires the following phases [3]:

1. Initialize $r_0 = m$ (the residual) and $k = 1$ (the index number of IMF).
2. Extract the k^{th} IMF (sifting process):
 - a. Initialize $h_0 = r_{k-1}$ and $j = 1$.
 - b. $j=1$ Extract the local minima and maxima of h_{j-1} .
 - c. Compute the upper envelope and lower envelope functions x_{j-1} and y_{j-1} by interpolating, respectively, the local minima and local maxima of h_{j-1} .
 - d. Compute the mean envelope: $m_{j-1} = (x_{j-1} + y_{j-1})/2$
 - e. Update $h_j = h_{j-1} - m_{j-1}$ and $j = j + 1$.
 - f. Calculate the stopping criterion: $SD(j) = \frac{1}{M \times N} \sum_{m=1}^M \sum_{t=0}^T \frac{(h_{j-1} - h_j)^2}{h_{j-1}^2 + \epsilon}$ where ϵ is a (weak) term eliminating any divisions by zero.
 - g. Decision: repeat steps (b) through (f) until $SD_j < SD_{max}$ and then put $d_k = h_j$ (k^{th} IMF).
3. Update the residue $r_k = r_{k-1} - d_k$.
4. Repeat steps 1–3 with $k = k + 1$ until the number of extrema in r_k is less than 2.

When the decomposition is achieved, we can write the signal in the following form:

$$I = \sum_{k=1}^P IMF_k + r_{P+1}$$

The stopping criterion is valid if SD does not exceed SD_{max} (certain predefined threshold), we use SD_{max} between 0.2 and 0.5 because this value gives satisfactory results in practice.

Figure 1 presents an example of the BEMD decomposition of the original texture image as Figure 1(a), this image is decomposed into three IMFs in Figures 1(b) to 1(d) and the residue in Figure 1(e), which illustrate a multiscale decomposition from high frequencies to low frequencies of the original image. However, a real obstacle to the implementation of this method is the computational complexity, most of which is consumed in creating the upper and lower envelopes by interpolated functions, like the radial basis functions (RBF) [2]. To solve this problem, some works have been proposed with a less expensive technique, such as using Delaunay triangulation [15], finite elements [16] or by utilizing a filter to obtain the upper and lower envelopes [17]. In the same context, Bhuiyan *et al.* [18] suggested using the statistical filters Max and Min accompanied by a smoothing operator repeated several times when generating the upper and lower envelopes, but there are several limitations such as: determining the correct filter size and the number of iterations of the smoothing operator.

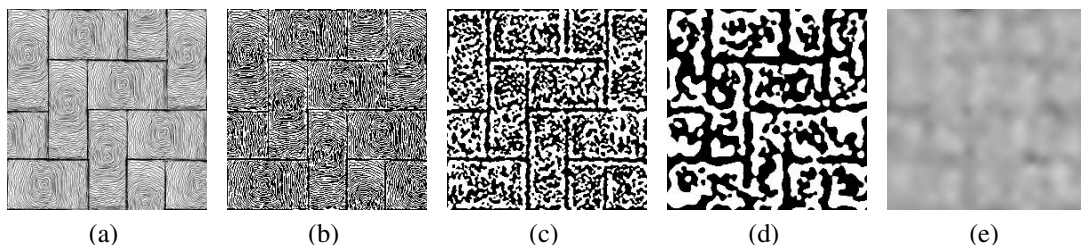


Figure 1. Example of BEMD decomposition of texture image: (a) original image, (b) IMF 1, (c) IMF 2, (d) IMF 3, and (e) residue

The BEMD using compactly supported radial basis functions (BEMD-CSRBF) [19] produces good results in terms of computational complexity and BEMD decomposition quality, particularly for the first IMFs. However, using a fixed support size for CSRBF functions in BEMD makes extracting low frequencies (last

IMFs) difficult. Especially since this decomposition is iterative, and each iteration produces a different number of extrema and a different distribution in space. Also, the number of extrema decreases after each IMF is extracted. Which makes using a fixed support size to extract all IMFs inefficient.

In this paper, we suggested an approach to adjust the support size during the BEMD algorithm. To extract the first IMF, we determine the CSRBF function support size (initial support) based on one of the distances in [18], because it is derived based on the distribution of the extrema. Considering that the extrema continuously reduce during the decomposition process, we just double the size of the initial support after extracting each IMF without the need to recalculate previous distances, thus avoiding increasing the complexity of the computation. This approach demonstrates enhanced quality in the BEMD-CSRBF decomposition and proves its efficacy when compared to other BEMD decomposition methods, both in terms of the quality of IMFs and the complexity of computations.

2. METHOD

2.1. Compactly supported radial basis functions

As our research is founded on the employment of the CSRBFs in the BEMD algorithm, the present study aims to explicate the characteristics of CSRBF functions belonging to this specific category. Notably, a family of radial basis functions with compact support was first introduced in the mid-1990s, as evidenced by the works of Wu in 1995 [20], and Wendland in 1999 [21]. It should be noted that there are other types of CSRBF functions [22], [23].

Generally, a basis radial function with compact support is given by the expression [24]:

$$\phi_{l,k}(r) = (1-r)_+^k p(r) \quad k \geq 1 \quad (1)$$

with

$$(1-r)_+^k = \begin{cases} (1-r)^k & r \in [0, 1] \\ 0 & r > 1 \end{cases} \quad (2)$$

where $p(r)$ is one of the polynomials prescribed by Wu or Wendland, the indices l and $2k$ represent respectively the space dimension and smoothness of the function.

The Table 1 contains some functions of Wu and Wendland. The difficulty with using CSRBFs is the size of the support. In the following, we look at the influence of the support size on the BEMD decomposition, especially since the extrema to be interpolated are reduced during the BEMD. We used the Wendland function $\varphi_{3,1}$ used in [19] as the CSRBF function.

Table 1. CSRBF functions of Wu and Wendland

	Smoothness	SPD
Wu functions		
$\psi_{1,3}(r) = (1-r)_+^6(5r^5 + 30r^4 + 72r^3 + 82r^2 + 36r + 6)$	\mathbb{C}^4	\mathbb{R}^3
$\psi_{2,3}(r) = (1-r)_+^5(5r^4 + 25r^3 + 48r^2 + 40r + 8)$	\mathbb{C}^2	\mathbb{R}^3
$\psi_{3,3}(r) = (1-r)_+^4(5r^3 + 20r^2 + 29r + 16)$	\mathbb{C}^0	\mathbb{R}^3
Wendland functions		
$\varphi_{3,1}(r) = (1-r)_+^4(4r + 1)$	\mathbb{C}^2	\mathbb{R}^3
$\varphi_{3,2}(r) = (1-r)_+^6(35r^2 + 18r + 3)$	\mathbb{C}^4	\mathbb{R}^3
$\varphi_{3,3}(r) = (1-r)_+^8(32r^3 + 25r^2 + 8r + 1)$	\mathbb{C}^6	\mathbb{R}^3

2.2. BEMD-CSRBF with adjusting the support size

To determine the size of support for the CSRBF function for the first IMF, we chose one of the distances used in [18] as the support size to ensure that each extrema center of the image's support contains other extrema points. As mentioned in [18], in order to determine the 4 distances, we must first extract the local maximal and the local minimal from the image, we calculate the Euclidean distance between each local maximal element and its nearest maximal element. Subsequently, we generate a table of distances called adjacent maximal distance array (T_{dmaxA}). Likewise, we calculate the table of adjacent minimal distance array (T_{dminA}). finally, the size of the support is chosen from these distances.

$$w = d_1 = \min \{ \min \{ T_{dmaxA} \}, \min \{ T_{dminA} \} \} \quad (3)$$

$$w = d_2 = \max \{ \min \{ TdmaxA \}, \min \{ TdminA \} \} \tag{4}$$

$$w = d_3 = \min \{ \max \{ TdmaxA \}, \max \{ TdminA \} \} \tag{5}$$

$$w = d_4 = \max \{ \max \{ TdmaxA \}, \max \{ TdminA \} \} \tag{6}$$

Knowing that the extrema decrease progressively during the decomposition, we just multiply the initial support size by 2 after extracting each IMF. Then, from the second IMF, the support size is estimated without recalculating the prior distances or using a data partitioning approach, thus avoiding increasing the complexity of the computation. Then our method follows the following steps:

- i) Identify the extrema (both the maximal and the minimal) of our image I, using the neighborhood window approach to extract extrema points from 2D.
- ii) Determine the support size initial θ using one of distances in [18].
- iii) Generate the first IMF with a CSRBF function using the initial support size θ .
- iv) Generate the k-ieme IMF ($k \geq 2$) with support size equal to $2^{k-1} * \theta$.

Our research focuses on the interpolation procedure, specifically on adjusting the support size of the CSRBF function. To do this, we kept the same CSRBF function (Wendland function $\varphi_{3,1}$) that was used in [19]. In our BEMD approach, the distance d_4 was used as the initial support size for the CSRBF function. This decision was based on this distance's improved performance in comparison to other distances mentioned in [18], and limiting the maximal number of allowed iterations (MNAI) to 5 for each IMF in order to prevent overfitting. Finally, the standard deviation (SD) is used as the basic stopping criterion, with a limit of 0.5.

2.3. Evaluation

To evaluate the efficacy of our method, we first decomposed cameraman image using BEMD-CSRBF with an adjustable support size and compared it with traditional BEMD-CSRBF decomposition. This was done to see the impact of the adjusted support size on the number of extrema during the proposed BEMD and the power of extraction of low frequencies. In addition, to thoroughly evaluate our approach, we conducted a comparative analysis between the IMFs generated by the new BEMD method and those produced by alternative methods such as : FABEMD [18] and BEMD-VNW [25]. The selection of FABEMD and BEMD-VNW was based on their effectiveness and rapidity compared to other EBMD approaches. On the other hand, we chose the synthetic texture image (STI) because it enables us to evaluate the efficacy of the BEMD approach using the orthogonality index (OI). The OI was developed in order to evaluate the quality of IMFs [18]. This index's definition is as:

$$OI = \sum_{x=1}^M \sum_{y=1}^N \left(\frac{\sum_{i=1}^{K+1} \sum_{j=1}^{K+1} \text{BEMC}_i - \text{BEMC}_j}{\sum_{BEMC}^2(x,y)} \right) \tag{7}$$

We refer to the IMFs and the residue as bidimensional empirical multimodal components (BEMCs). A smaller OI value indicates an optimal decomposition with respect to local orthogonality. In general, OI values of 0.1 or less are often regarded as sufficient. However, the FABEMD is a BEMD approach that does away with the interpolation phase. The upper and lower envelopes are obtained from the image's extrema using order-statistics filter, with just one iteration for each IMF (MNAI=1). However, in order to prevent significant discontinuities, both envelopes need to have a smoothing operator applied multiple times, which increases the computation time. While fast BEMD based on variable neighborhood window method (BEMD-VNW) suggests replacing the square window used in the FABEMD approach with a disc window, which has an isotropic structure element window, considering that the isotropic structural element window is more compatible with the image's properties, adjacent maximal and minimal values are averaged to determine the appropriate size for the window.

3. RESULTS AND DISCUSSION

3.1. BEMD-CSRBF with adjusting the support size

In this section, we used the cameraman image of size 128×128 as a simulation image in Figure 2. Table 2 shows the development of extrema during the IMFs with a support size of 10 for the CSRBF function.

The results corresponding to a support size of 20 are represented below in Table 3. Table 2 shows that the development of the number of extrema (either the maximal or the minimal) remains stable, especially from the third IMF between 136 and 156 for maximal and between 119 and 121 for minimal, with an execution time of 10.30 seconds. At the size of support 20 as shown in Table 3, we find that the development of the number of extrema is faster, but in the last two IMFs, it remains stable with fewer extremes. with an increase in execution time (19.34 seconds), which is logical when we use a larger support size of the CSRBF functions in the interpolation phase.



Figure 2. Original image

Table 2. Number of extrema and execution time during BEMD decomposition with support size equal to 10

	Example in Arabic	
	Max	Min
IMF 1	656	637
IMF 2	214	199
IMF 3	156	121
IMF 4	136	119
Time	10.30 s	

Table 3. Number of extrema and execution time during BEMD decomposition with support size equal to 20

	Number of extrema	
	Max	Min
IMF1	708	694
IMF2	105	96
IMF3	53	53
IMF4	44	45
Time	19.34 s	

In both cases, the number of extrema is stable in the last IMFs due to a discontinuity of the signal using a fixed support size. Because the support no longer contains extrema for estimating the best envelopes (upper and lower). This influenced the extraction of low frequencies, as demonstrated in Figures 3 and 4. Figures 3(a) to 3(d) depict the IMFs extracted from the cameraman image with a fixed support size of 10, while Figures 4(a) to 4(d) display the IMFs extracted with a fixed support size of 20.

Table 4 displays the evolution of the number of extrema points, including both maximal and minimal values, as well as the time taken for the BEMD decomposition of the cameraman image using a novel method. This table shows how the number of extrema varies with each IMF, offering important insight into the performance and efficiency of the algorithm. Additionally, Figure 5 illustrates this image's BEMD decomposition, and Figures 5(a) to 5(d) show all of these IMFs.

According to Table 4, we observe that the number of extrema during BEMD is gradually decreasing from the first IMF (708 for maxima and 694 for minima) to the fourth IMF (9 for maxima and 10 for minima). This type of evolution allows us to extract the low frequencies, as we see in Figure 5. We also noted that the calculation time (12.19 seconds) remains acceptable, especially since we have ensured the extraction of low frequencies.

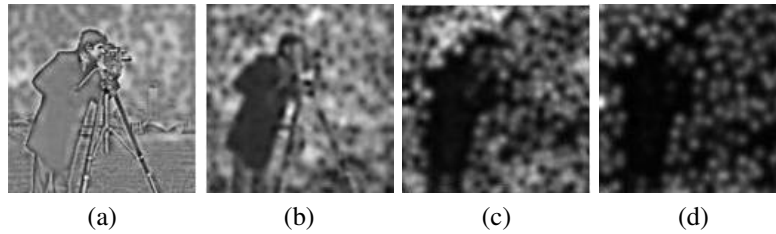


Figure 3. BEMD-CSRBF with a support size of 10 on (a) IMF 1, (b) IMF 2, (c) IMF 3, and (d) IMF 4

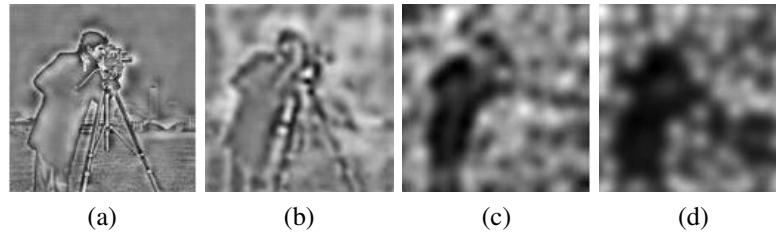


Figure 4. BEMD-CSRBF with a support size of 20 on (a) IMF 1, (b) IMF 2, (c) IMF 3, and (d) IMF 4

Table 4. Number of extrema and execution time during BEMD decomposition with adjusting support size

	Number of extrema	
	Max	Min
IMF1	708	694
IMF2	116	117
IMF3	27	29
IMF4	9	10
Time	12.19 s	

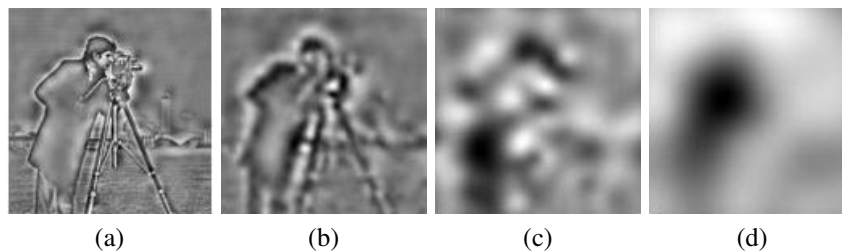


Figure 5. BEMD-CSRBF with adjusting support size: (a) IMF 1, (b) IMF 2, (c) IMF 3, and (d) IMF 4

3.2. Analyses and discussion using a synthetic texture image

In this section, we utilized a STI of size 256×256 pixels. The STI was generated by combining three synthetic component images (SCIs). Both the STI and SCIs are shown in Figure 6. We create each SCI by employing sinusoidal waves with slight variation in frequency in both the horizontal and vertical directions.

Figure 6(a) illustrates the higher frequencies (SCI 1), Figure 6(b) illustrates the middle frequencies (SCI 2), Figure 6(c) illustrates the low frequencies (SCI 3), and Figure 6(d) presents the STI. Table 5 presents the global mean of each component SCI and the OI values of the STI.

The STI in Figure 6(c) was used to apply a novel algorithm. Figures 7 to 9 demonstrate that IMFs resembled the original SCIs. Figure 7 shows the IMFs as shown in Figures 7(a) to 7(c) and their summation in Figure 7(d) resulting from the FABEMD. The IMFs of the STI as shown in Figures 8(a) to 8(c) and their summation in Figures 8(d) corresponding to BEMD-VNW are presented in Figure 8. And Figure 9 present the IMFs in Figures 9(a) to 9(c) and their summation in Figure 9(d) resulting from the proposed BEMD. The proposed BEMD generates 3 IMFs (SCI), which is the same number as the original STI. This indicates that the decomposition of the method is appropriate.

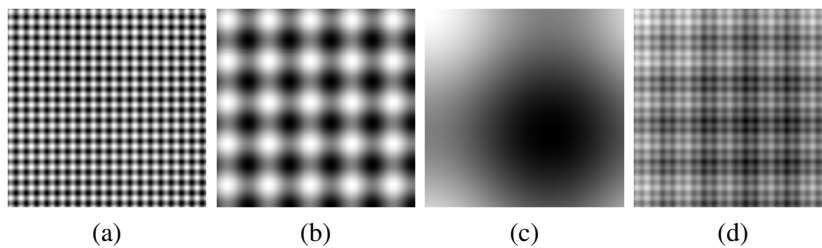


Figure 6. STI and their SCIs; (a) SCI-1, (b) SCI-2, (c) SCI-3, and (d) STI obtained by adding (a) to (c)

Table 5. Index of orthogonality and global mean of SCIs

	SCI 1	SCI 2	SCI 3
Global mean	0.0046	0.0622	-0.287
OI		0.0488	

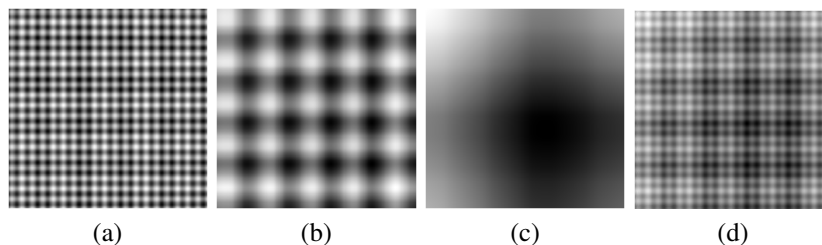


Figure 7. STI decomposition using FABEMD: (a) IMF 1, (b) IMF 2, (c) IMF 3, (d) STI obtained by adding (a) to (c)

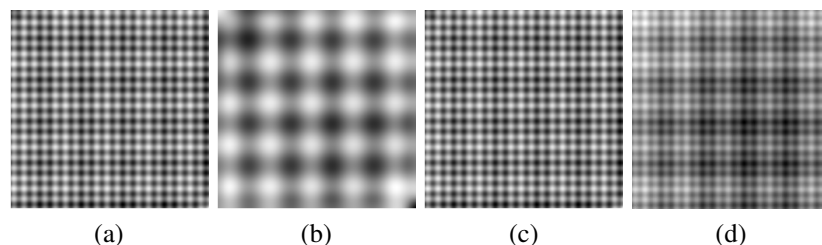


Figure 8. STI decomposition using BEMD based on variable neighborhood: (a) IMF 1, (b) IMF 2, (c) IMF 3, (d) STI obtained by adding (a) to (c)

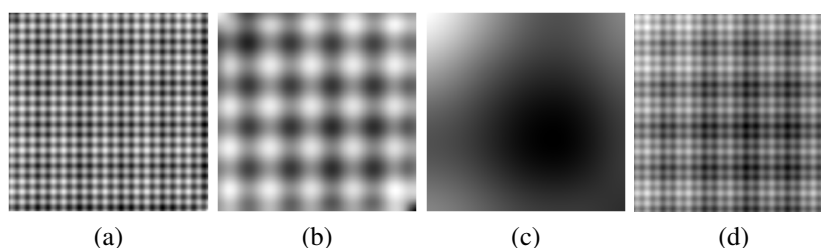


Figure 9. STI decomposition using proposed BEMD: (a) IMF 1, (b) IMF 2, (c) IMF 3, (d) STI obtained by adding (a) to (c)

To conduct a more thorough evaluation of the novel BEMD and two other BEMD methods, Table 6 presents the number of acquired IMFs, the time required, and the OI values of the decomposition of the STI for each algorithm. We observed that the number of IMFs remains 3 in the proposed BEMD and other methods of BEMD. This effectively supports the number of components (SCIs) of STI, indicating that they exhibit good decompositions. Compared to the execution time and OI values, we observe that the suggested approach has an improved execution time of 3.23 seconds and a more effectively OI value of 0.0975.

In general, these characteristics indicate that the proposed is an appropriate choice for the decomposition of the STI in Figure 1(d) in comparison with the FABEMD and BEMD-VNW algorithms, knowing that the OI values and time required for the corresponding novel method are less than those corresponding to other BEMD methods. which makes this method a favourable choice for various imagery applications, especially those focused on feature extraction, including image indexing and facial recognition.

Table 6. Comparing the proposed BEMD, FABEMD and BEMD-VNW for the STI, including the total number of BEMCs, total time needed, and OI

	Proposed BEMD	FABEMD	BEMD-VNW
Total no. of IMFs	3	3	3
Total time (seconds)	3.23	4.09	3.78
OI	0.0975	0.1102	0.1049

4. CONCLUSION

This article presents an improvement to the BEMD-CSRBF algorithm for efficient low frequency extraction (the last IMFs). This method is based on adjusting the support size of the CSRBF function in the BEMD algorithm. To extract the first IMF, we determine the support size of the CSRBF function based on the extrema distribution, and then the other IMFs are extracted using a dynamic support size based on the initial support size. This approach demonstrates improved quality in the BEMD-CSRBF decomposition and proves its effectiveness compared to other BEMD decomposition methods, both in terms of quality of IMFs and computational complexity. Future research will focus on the CSRBF function's adaptive choice depending on the image used and its frequency content.




REFERENCES

- [1] N. E. Huang *et al.*, "The empirical mode decomposition and the Hilbert spectrum for nonlinear and non-stationary time series analysis," *Proceedings of the Royal Society of London. Series A: Mathematical, Physical and Engineering Sciences*, vol. 454, no. 1971, pp. 903–995, Mar. 1998, doi: 10.1098/rspa.1998.0193.
- [2] P. Flandrin, G. Rilling, and P. Goncalves, "Empirical mode decomposition as a filter bank," *IEEE Signal Processing Letters*, vol. 11, no. 2, pp. 112–114, Feb. 2004, doi: 10.1109/LSP.2003.821662.
- [3] J. -C. Nunes, Y. Bouaoune, E. Delechelle, O. Niang, and P. Bunel, "Image analysis by bidimensional empirical mode decomposition," *Image and Vision Computing*, vol. 21, no. 12, pp. 1019–1026, Nov. 2003, doi: 10.1016/S0262-8856(03)00094-5.
- [4] Sumanto, A. Buono, K. Priandana, B. P. Silalahi, and E. S. Hendrastuti, "Texture analysis of citrus leaf images using BEMD for Huanglongbing disease diagnosis," *Jurnal Online Informatika*, vol. 8, no. 1, pp. 115–121, Jun. 2023, doi: 10.15575/join.v8i1.1075.
- [5] Z. Yang, D. Qi, and L. Yang, "Signal period analysis based on Hilbert-Huang transform and its application to texture analysis," in *Proceedings - Third International Conference on Image and Graphics*, 2004, pp. 430–433, doi: 10.1109/icig.2004.129.
- [6] A. Sabri, M. Karoud, and H. T. A. Aarab, "An efficient image retrieval approach based on spatial correlation of the extrema points of the IMEs," *Review Literature And Arts Of The Americas*, vol. 3, no. November, pp. 597–605, 2008.




- [7] L. Yang, M. Zhang, J. Cheng, T. Zhang, and F. Lu, "Retina images classification based on 2D empirical mode decomposition and multifractal analysis," *Heliyon*, vol. 10, no. 6, p. e27391, Mar. 2024, doi: 10.1016/j.heliyon.2024.e27391.
- [8] K. Amiri, M. Imani, and H. Ghassemian, "Empirical mode decomposition based morphological profile for hyperspectral image classification," in *2023 6th International Conference on Pattern Recognition and Image Analysis (IPRIA)*, Feb. 2023, pp. 1–6, doi: 10.1109/IPRIA59240.2023.10147181.
- [9] R. Zhuo, Y. Guo, B. Guo, B. Liu, and F. Dai, "Two-dimensional compact variational mode decomposition for effective feature extraction and data classification in hyperspectral imaging," *Journal of Applied Remote Sensing*, vol. 17, no. 04, p. 044517, Dec. 2023, doi: 10.1117/1.jrs.17.044517.
- [10] Z. Benli and S. G. Ak, "A novel approach for breast ultrasound classification using two-dimensional empirical mode decomposition and multiple features," *Experimental Biomedical Research*, vol. 7, no. 1, pp. 27–38, Jan. 2024, doi: 10.30714/j-ebr.2024.205.
- [11] M. Arrazaki, A. Sabri, M. Zohry, and T. Zougari, "Adaptive image watermarking using bidimensional empirical mode decomposition," *Bulletin of Electrical Engineering and Informatics*, vol. 12, no. 5, pp. 2955–2963, Oct. 2023, doi: 10.11591/eei.v12i5.4688.
- [12] J. Hu, M. Dai, X. Wang, Q. Xie, and D. Zhang, "Robust 3D watermarking with high imperceptibility based on EMD on surfaces," *The Visual Computer*, vol. 40, no. 11, pp. 7685–7700, Nov. 2023, doi: 10.1007/s00371-023-03201-5.
- [13] G. H. Nguyen, Y. T. H. Hua, and L. V. Dang, "MRI brain tumor segmentation using bidimensional empirical mode decomposition and morphological operations," in *Lecture Notes in Networks and Systems*, vol. 752 LNNS, 2023, pp. 1–11.
- [14] F. Ghazil, A. Benkuider, F. Ayoub, M. Zraidi, and K. Ibrahim, "Fractal analysis to BEMD's IMFs: application CT-scan," in *2023 6th International Conference on Advanced Communication Technologies and Networking (CommNet)*, Dec. 2023, pp. 1–7, doi: 10.1109/CommNet60167.2023.10365292.
- [15] C. Damerval, S. Meignen, and V. Perrier, "A fast algorithm for bidimensional EMD," *IEEE Signal Processing Letters*, vol. 12, no. 10, pp. 701–704, Oct. 2005, doi: 10.1109/LSP.2005.855548.
- [16] Y. Xu, B. Liu, J. Liu, and S. Riemenschneider, "Two-dimensional empirical mode decomposition by finite elements," in *Proceedings of the Royal Society A: Mathematical, Physical and Engineering Sciences*, Oct. 2006, vol. 462, no. 2074, pp. 3081–3096, doi: 10.1098/rspa.2006.1700.
- [17] Q. Xie, J. Hu, X. Wang, Y. Du, and H. Qin, "Novel optimization-based bidimensional empirical mode decomposition," *Digital Signal Processing*, vol. 133, p. 103891, Mar. 2023, doi: 10.1016/j.dsp.2022.103891.
- [18] S. M. A. Bhuiyan, R. R. Adhami, and J. F. Khan, "Fast and adaptive bidimensional empirical mode decomposition using order-statistics filter based envelope estimation," *EURASIP Journal on Advances in Signal Processing*, vol. 2008, no. 1, p. 728356, Dec. 2008, doi: 10.1155/2008/728356.
- [19] M. Arrazaki and T. Zougari, "Using compactly supported radial basis function to speed up BEMD decomposition time (in French: L'utilisation de fonction radiale de base à support compact pour accélérer le temps de décomposition BEMD)," *IOSR journal of VLSI and Signal Processing*, vol. 4, no. 3, pp. 24–29, 2014, doi: 10.9790/4200-04312429.
- [20] Z. Wu, "Compactly supported positive definite radial functions," *Advances in Computational Mathematics*, vol. 4, no. 1, pp. 283–292, Dec. 1995, doi: 10.1007/BF03177517.
- [21] H. Wendland, "Piecewise polynomial, positive definite and compactly supported radial functions of minimal degree," *Advances in Computational Mathematics*, vol. 4, no. 1, pp. 389–396, Dec. 1995, doi: 10.1007/BF02123482.
- [22] M. Buhmann, "A new class of radial basis functions with compact support," *Mathematics of Computation*, vol. 70, no. 233, pp. 307–318, Mar. 2000, doi: 10.1090/S0025-5718-00-01251-5.
- [23] T. Gneiting, "Compactly supported correlation functions," *Journal of Multivariate Analysis*, vol. 83, no. 2, pp. 493–508, Nov. 2002, doi: 10.1006/jmva.2001.2056.
- [24] G. E. Fasshauer, *Meshfree approximation methods with MATLAB*. World Scientific Publishing Company, 2007.
- [25] X. Ma, X. Zhou, and F. An, "Fast bi-dimensional empirical mode decomposition (BEMD) based on variable neighborhood window method," *Multimedia Tools and Applications*, vol. 78, no. 7, pp. 8889–8910, Apr. 2019, doi: 10.1007/s11042-018-6629-6.

BIOGRAPHIES OF AUTHORS




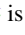


Mohammed Arrazaki    received his Ph.D. degree in 2021 for his research work in applied mathematics from Faculty of Sciences Tetouan, Morocco. His fields of interest are applied mathematics, image analysis, image processing, machine learning, and deep learning. He can be contacted at email: rezaki_mohamed@hotmail.com.







Othman El Ouahabi    is a Ph.D. student in National School of Applied Sciences of Tangier, Morocco. His fields of interest are image processing, machine learning, and deep neural networks. He can be contacted at email: othman.elouahabi1@etu.uae.ac.ma.



Mohamed Zohry     is a professor at the Faculty of Sciences Tetouan, Morocco. He received his Ph.D. degree in 1990 from Faculty of Sciences, Rabat, Morocco. And Ph.D. in 1996 at Granada University (Spain). His research areas include analysis, geometry and topology, number theory, applied mathematics, statistics, and probability theory. He can be contacted at email: zohry@hotmail.fr.



Adel Babbah     is a professor at the Polydisciplinary Faculty of Larache, Morocco. He received his Ph.D. degree in 2016 from Faculty of Sciences, Tetouan, Morocco. His research areas include functional analysis, operators theory, applied mathematics, and Complex analysis. He can be contacted at email: adel.groupe@gmail.com.